ROYAL INSTITUTE
OF TECHNOLOGY

Rayleigh-Bénard convection

Maja Sandberg
Götgatan 78
11830 Stockholm

+46707395394
majasa@kth.se

Niclas Berg
Sarvstigen 3
18130 Lidingö

+46735431430
niber@kth.se

Gustav Johnsson
Kungshamra 82
17070 Solna

+46735128711
gusjoh@kth.se

16th May 2011

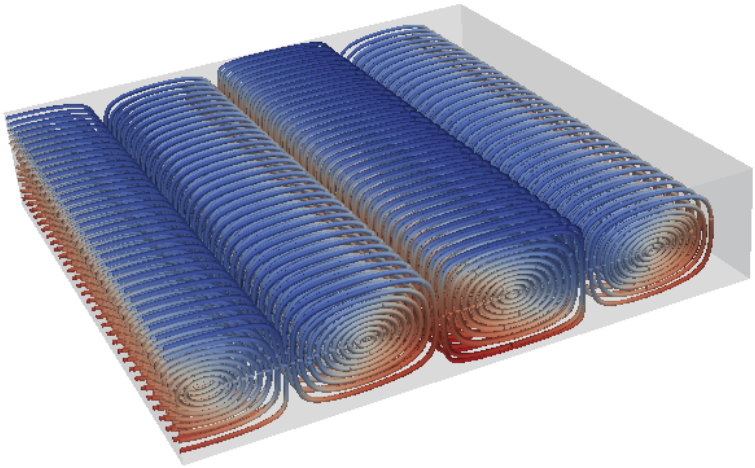

Bachelor degree project, SA104X, KTH Mechanics
Supervisor: Philipp Schlatter, pschlatt@mech.kth.se

Abstract

This report considers Rayleigh-Bénard convection, i.e. the flow between two large parallel plates where the lower one is heated. The change in density due to temperature variations gives rise to a flow generated by buoyancy. This motion is opposed by the viscous forces in the fluid. The balance between these forces determines whether the flow is stable or not and the goal of this report is to find a condition giving this limit as well as analyzing other aspects of the flow.

The starting point of the analysis is the incompressible Navier-Stokes equations and the thermal energy equation upon which the Boussinesq approximation is applied. Using linear stability analysis a condition for the stability is obtained depending solely on a non-dimensional parameter, called the Rayleigh number, for a given wavenumber k. This result is confirmed to be accurate after comparison with numerical simulations using a spectral technique.

Further non-linear two- and three-dimensional simulations are also performed to analyze different aspects of the flow for various values of the Rayleigh number.

Sammanfattning

I denna rapport betraktas Rayleigh-Bénardkonvektion, det vill säga flödet mellan två stora parallella plattor där den undre plattan värms. Eftersom densiteten i vätskan mellan plattorna beror av temperaturen kommer ett flöde att uppstå på grund av flytkraften, som i sin tur motverkas av de viskösa krafterna i vätskan. Förhållandet mellan dessa krafter kommer att bestämma huruvida flödet är stabilt eller inte. Målet med denna rapport är att hitta ett villkor som ger gränsen mellan dessa fall samt att undersöka andra egenskaper hos flödet.

Analysen utgår från Navier-Stokes ekvationer för inkompressibelt flöde samt ekvationen för den termiska energin, på vilka Boussinesqs approximation tillämpas. Med hjälp av linjär stabilitetsanalys fås ett stabilitetsvillkor som endast beror av ett dimensionslöst tal, kallat Rayleigh-talet, för ett givet vågtal, k. Detta resultat bekräftas även med numeriska simuleringar som utfördes med en spektral metod.

Vidare utfördes även icke-linjära simulationer i två och tre dimensioner för att undersöka olika aspekter hos flödet för olika värden på Rayleigh-talet.

Contents

1 Introduction

Rayleigh-Bénard convection is a type of flow that is only driven by differences in density due to a temperature gradient. The Rayleigh-Bénard convection occurs in a volume of fluid that is heated from below. In the case studied in this report the fluid is kept between two enclosing parallel plates and the lower plate is kept at a higher temperature. The fluid near the lower plate will get a higher temperature and therefore a lower density than the rest of the fluid. Gravity will make the colder and heavier fluid at the top sink but this is opposed by the viscous force in the fluid. It is the balance between these two forces that determines if convection will occur or not. If the temperature gradient, and thus the density gradient, is large enough the gravitational forces will dominate and instability will occur. It is the limit of instability and the occuring flow patterns that are investigated in this report through both numerical and analytical methods.

1.1 History

In 1900 Henri Bénard made experiments on the instability of a thin layer ($\leq$ 1mm) of fluid heated from below. The convection of Bénards experiment involved surface tension and thermo-capillary convection, which is called Bénard-Marangoni convection, whilst Rayleigh-Bénard convection depends solely on a temperature gradient. But the experiment made by Bénard inspired Lord Rayleigh (J.W. Strutt) who in 1916 derived the theoretical demands for the temperature gradient convection, hence the combined name. Rayleigh showed that instability occurs when the temperature gradient ΔT is large enough to make the non-dimensional Rayleigh number, Ra, exceed a certain critical value. The Rayleigh number is defined as

$$\mathrm{Ra} = \frac{\alpha \Delta T g h^3}{\nu \kappa},$$

where ΔT is the temperature gradient, α is the thermal expansion coefficient, g is the acceleration due to gravity, h is the distance between the plates, ν is the kinematic viscosity and κ is the thermal diffusivity.

2 Theory

In this section the governing conservation laws for a fluid will be formulated such as the ones for mass, momentum and energy. Various approximations will then be applied to achieve a set of equations known as the Boussinesq equations.

2.1 Governing equations

The flow is governed by the conservation of three basic quantities, i.e. mass, momentum and energy, each yielding a conservation equation. The conservation of mass states that [2]

$$\frac{1}{\rho}\frac{\mathrm{D}\rho}{\mathrm{D}t} + \nabla \cdot \boldsymbol{u} = 0, \tag{1}$$

where ρ is the density, $\boldsymbol{u}$ is the velocity and $\mathrm{D}/\mathrm{D}t$ denotes the material derivative, which can be expressed symbolically as

$$\frac{\mathrm{D}}{\mathrm{D}t} = \frac{\partial}{\partial t} + \boldsymbol{u} \cdot \nabla.$$

If the flow is incompressible, i.e. the density of any given fluid particle does not vary throughout the flow $D\rho/Dt = 0$ and (1) yields

$$\nabla \cdot \boldsymbol{u} = 0. \tag{2}$$

The law of momentum conservation yields the equation

$$\rho\frac{\mathrm{D}u_i}{\mathrm{D}t} = \rho g_i + \frac{\partial \tau_{ij}}{\partial x_j},$$

where g_i is the gravitational acceleration and τ_{ij} is the stress tensor composed of viscous stresses and normal stresses caused by the pressure. For incompressible flow one can show that it takes the form

$$\rho\frac{\mathrm{D}\boldsymbol{u}}{\mathrm{D}t} = -\nabla p + \rho\boldsymbol{g} + \mu\nabla^2\boldsymbol{u}, \tag{3}$$

which is known as the incompressible Navier-Stokes equations. Here, p denotes the pressure in the fluid and μ is the viscosity.

Lastly, the energy conservation states that

$$\rho\frac{\mathrm{D}e}{\mathrm{D}t} = -\nabla \cdot \boldsymbol{q} - p\nabla \cdot \boldsymbol{u} + \phi, \tag{4}$$

where e is the thermal energy density, $\boldsymbol{q}$ is the heat flux density and ϕ is the rate of dissipation through viscous effects per unit volume. For incompressible flow it can be calculated through $\phi = 2\mu e_{ij}e_{ij}$ where e_{ij} is the strain rate tensor. The strain rate tensor contains the deformations of the fluid particles in the flow and is defined as

$$e_{ij} = \frac{1}{2}\left[\frac{\partial u_i}{\partial x_j} + \frac{\partial u_j}{\partial x_i}\right].$$

The set of equations (2), (3) and (4) describe the behavior and properties of an incompressible flow and are the starting point for the analysis in this report. In the next section various approximations will be applied in order to simplify these equations.

2.2 Boussinesq's approximation

The so-called Boussinesq approximation was first proposed by Joseph Valentin Boussinesq (1842-1929) during the second part of the 19th century. His essential observation was that in a bouyancy driven flow the density variations can be neglected everywhere in the momentum equation except in the gravitation term. This will be applied to simplify the Navier-Stokes equations and further assumptions will be made to rewrite the thermal energy equation.

2.2.1 Navier-Stokes equations

Assume that the density variations in the fluid are small in comparison with the velocity gradients, then we can deduce from the mass conservation (1) that

$$\nabla \cdot \boldsymbol{u} \approx 0. \tag{5}$$

Assume further that the pressure and density can both be decomposed into a background field in hydrostatic equilibrium and a perturbation, thus taking the form

$$p = p_0(y) + p'(\boldsymbol{x}, t), \qquad \rho = \rho_0 + \rho'(\boldsymbol{x}, t),$$

where $p_0(y)$ and ρ_0 represents the background field. For the hydrostatic case, $\boldsymbol{u} = \boldsymbol{0}$ and Navier-Stokes equation (3) yields

$$\nabla p_0 = \rho_0 \boldsymbol{g}. \tag{6}$$

Subtracting this from the Navier-Stokes equations (3) and dividing by ρ_0 gives

$$\left(1 + \frac{\rho'}{\rho_0}\right) \frac{\mathrm{D}\boldsymbol{u}}{\mathrm{D}t} = -\frac{1}{\rho_0}\nabla p' + \frac{\rho'}{\rho_0}\boldsymbol{g} + \nu \nabla^2 \boldsymbol{u}, \tag{7}$$

where $\nu = \mu/\rho_0$ is the kinematic viscosity.

For small values of ρ'/ρ_0, the left hand side of the equation reduces to $\mathrm{D}\boldsymbol{u}/\mathrm{D}t$. The bouyancy term $\rho'\boldsymbol{g}/\rho_0$ in the right hand side though cannot be neglected since the gravity is strong enough to make the density variation relevant [3].

With these assumptions, the following equation is obtained

$$\frac{\mathrm{D}\boldsymbol{u}}{\mathrm{D}t} = -\frac{1}{\rho_0}\nabla p' + \frac{\rho'}{\rho_0}\boldsymbol{g} + \nu \nabla^2 \boldsymbol{u}. \tag{8}$$

2.2.2 Thermal energy equation

The thermal energy equation (4),

$$\rho \frac{\mathrm{D}e}{\mathrm{D}t} = -\nabla \cdot \boldsymbol{q} - p \nabla \cdot \boldsymbol{u} + \phi, \tag{9}$$

will now be treated. It can be shown that for the cases where the Boussinesq approximation is valid, the viscous dissipation rate ϕ only gives a negligable contribution to the thermal energy [3] and will thus not be included.

The assumption made in the last section about the small density variations is not applicable here [2], we must instead use the full mass conservation (1). Multiplying this relation by p and rearranging yields

$$-p\nabla \cdot \boldsymbol{u} = \frac{p}{\rho}\frac{\mathrm{D}\rho}{\mathrm{D}t}.$$

Now assume that the density variations are small enough to be approximated by a linear temperature dependency of the form

$$\rho = \rho_0(1 - \alpha(T - T_0)), \tag{10}$$

where $\alpha = -1/\rho_0 \cdot (\partial\rho/\partial T)_p$.

Assume further that the fluid molecules do not interact with each other, hence we can use the ideal gas approximation $p = \rho RT$ and $R = C_p - C_v$, yielding

$$-p\nabla \cdot \boldsymbol{u} \approx \frac{p}{\rho}\left(\frac{\partial\rho}{\partial T}\right)_p \frac{\mathrm{D}T}{\mathrm{D}t} = -\frac{p}{T}\frac{\mathrm{D}T}{\mathrm{D}t} = -\rho(C_p - C_v)\frac{\mathrm{D}T}{\mathrm{D}t}.$$

Using that for a perfect gas $e = C_v T$ the thermal energy equation becomes

$$\rho C_p \frac{\mathrm{D}T}{\mathrm{D}t} = -\nabla \cdot \boldsymbol{q}.$$

Fourier's law states that

$$\boldsymbol{q} = -k\nabla T,$$

where k is the thermal conductivity.

The thermal energy equation (9) finally becomes

$$\frac{\mathrm{D}T}{\mathrm{D}t} = \kappa\nabla^2 T, \tag{11}$$

where we have introduced the thermal diffusivity $\kappa \equiv k/\rho C_p$.

3 Problem formulation

Consider two infinitly large plates with a distance h between them, see figure 1. The lower and upper plate have a temperature of T_0 and T_1 respectively, such that $T_0 > T_1$. Between the plates we have a fluid with density ρ, kinematic viscosity ν, thermal diffussivity κ and thermal expansion coefficient α. The domain, Ω, in which this fluid is situated is defined as

$$\Omega : 0 < y < h, -\infty < x, z < \infty.$$

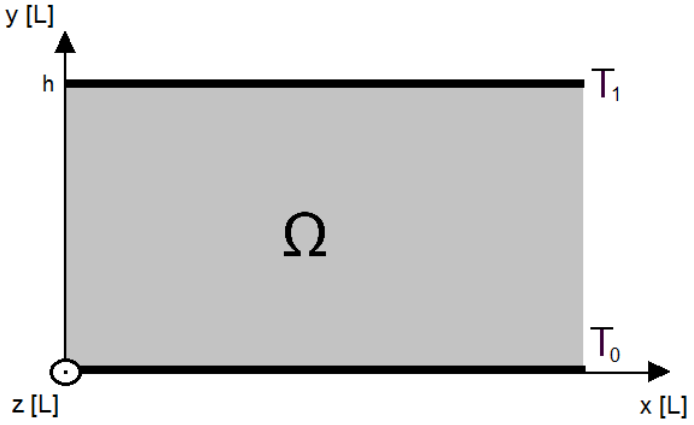

Figure 1: Problem domain.

The fluid obeys the equations that we have derived in the earlier sections. These governing equations are

$$\begin{cases} \dfrac{\mathrm{D}\boldsymbol{u}}{\mathrm{D}t} = -\dfrac{1}{\rho_0}\nabla p + \dfrac{\rho}{\rho_0}\boldsymbol{g} + \nu\nabla^2\boldsymbol{u}, & x, y, z \in \Omega, t > 0, \\ \dfrac{\mathrm{D}T}{\mathrm{D}t} = \kappa\nabla^2 T, & x, y, z \in \Omega, t > 0, \\ \nabla \cdot \boldsymbol{u} = \boldsymbol{0}, \\ \rho = \rho_0(1 - \alpha(T - T_0)). \end{cases} \tag{12}$$

As boundary conditions we use that we have a constant temperature at the lower and upper wall along with no-slip conditions,

$$\begin{cases} T(\boldsymbol{x}, t)|_{y=0} = T_0, & -\infty < x, z < \infty, t > 0, \\ T(\boldsymbol{x}, t)|_{y=h} = T_1, & -\infty < x, z < \infty, t > 0, \\ \boldsymbol{u}(\boldsymbol{x}, t)|_{y=0} = \boldsymbol{u}(\boldsymbol{x}, t)|_{y=h} = \boldsymbol{0}, & -\infty < x, z < \infty, t > 0, \end{cases} \tag{13}$$

and as initial conditions we have that the fluid is at rest and that the temperature in linearly distributed,

$$\begin{cases} T(y, t)|_{t=0} = T_0 + \frac{y}{h}(T_1 - T_0), & x, y, z \in \Omega, \\ \boldsymbol{u}(\boldsymbol{x}, t)|_{t=0} = \boldsymbol{0}, & x, y, z \in \Omega. \end{cases} \tag{14}$$

4 Non-dimensionalization

To be able to further analyze this problem and find the characteristic quantities, we introduce dimensionless parameters by making the substitutions

$$p = U^2\rho_0\frac{\nu}{\kappa}\bar{p}, \quad \boldsymbol{u} = U\bar{\boldsymbol{u}}, \quad T = \Delta T\bar{T} + T_0, \quad \boldsymbol{x} = h\bar{\boldsymbol{x}}, \quad t = \frac{h}{U}\bar{t}, \tag{15}$$

where all the quantities with a bar are dimensionless. Here we have introduced a velocity scale, U, a length scale, h, a dynamic pressure scale, $U^2\rho_0\nu/\kappa$, a time scale, h/U, and a temperature scale, $\Delta T = T_0 - T_1$.

From the coordinate transformation we get that

$$\nabla = \frac{1}{h}\bar{\nabla}, \quad \rho = \rho_0(1 - \alpha\Delta T\bar{T}), \quad \frac{\partial}{\partial t} = \frac{U}{h}\frac{\partial}{\partial \bar{t}}, \quad \frac{\mathrm{D}\boldsymbol{u}}{\mathrm{D}t} = \frac{U^2}{h}\frac{D\bar{\boldsymbol{u}}}{D\bar{t}}, \tag{16}$$

which inserted into (12) yields

$$\begin{cases} \dfrac{U^2}{h}\dfrac{\mathrm{D}\bar{\boldsymbol{u}}}{\mathrm{D}\bar{t}} & = -\dfrac{U^2\nu}{h\kappa}\bar{\nabla}\bar{p} + \alpha\Delta T\bar{T}\boldsymbol{g} + \dfrac{U\nu}{h^2}\bar{\nabla}^2\bar{\boldsymbol{u}}, \\ \dfrac{\Delta T U}{h}\dfrac{\mathrm{D}\bar{T}}{\mathrm{D}\bar{t}} & = \dfrac{\Delta T\kappa}{h^2}\bar{\nabla}^2\bar{T}. \end{cases}$$

By rearranging and identifying non-dimensional coefficients we find that

$$\begin{cases} \dfrac{\mathrm{D}\bar{\boldsymbol{u}}}{\mathrm{D}\bar{t}} & = -\mathrm{Pr}\bar{\nabla}\bar{p} + \mathrm{Ri}\alpha\Delta T\bar{T}\boldsymbol{e}_y + \dfrac{1}{\mathrm{Re}}\bar{\nabla}^2\bar{\boldsymbol{u}}, \quad 0 < \bar{y} < 1, -\infty < \bar{x}, \bar{z} < \infty, \bar{t} > 0, \\ \dfrac{\mathrm{D}\bar{T}}{\mathrm{D}\bar{t}} & = \dfrac{1}{\mathrm{Pe}}\bar{\nabla}^2\bar{T}, \qquad\qquad\qquad\qquad\quad 0 < \bar{y} < 1, -\infty < \bar{x}, \bar{z} < \infty, \bar{t} > 0, \end{cases} \tag{17}$$

where

$$\mathrm{Pr} = \frac{\nu}{\kappa}, \quad \mathrm{Ri} = \frac{gh}{U^2}, \quad \mathrm{Re} = \frac{Uh}{\nu}, \quad \mathrm{Pe} = \mathrm{Re}\cdot\mathrm{Pr} = \frac{Uh}{\kappa},$$

are the Prandtl, Richardson, Reynolds and Péclet numbers. This form will be used for calculation purposes. To analyse stability, however, we rewrite this into another form by introducing a different velocity scale

$$U_\kappa = \frac{\kappa}{h},$$

which transforms the equations to

$$\begin{cases} \dfrac{1}{\mathrm{Pr}}\dfrac{\mathrm{D}\bar{\boldsymbol{u}}}{\mathrm{D}\bar{t}} & = -\bar{\nabla}\bar{p} + \mathrm{Ra}\bar{T}\boldsymbol{e}_y + \bar{\nabla}^2\bar{\boldsymbol{u}}, \quad 0 < \bar{y} < 1, -\infty < \bar{x}, \bar{z} < \infty, \bar{t} > 0, \\ \dfrac{\mathrm{D}\bar{T}}{\mathrm{D}\bar{t}} & = \bar{\nabla}^2\bar{T}, \qquad\qquad\quad 0 < \bar{y} < 1, -\infty < \bar{x}, \bar{z} < \infty, \bar{t} > 0, \end{cases} \tag{18}$$

where Ra is the Rayleigh number defined by

$$\mathrm{Ra} = \frac{\alpha \Delta T g h^3}{\nu \kappa},$$

and its physical interpretation is the ratio between the bouyancy and viscous forces since

$$\frac{\text{Bouyancy force}}{\text{Viscous force}} \sim \frac{g\rho}{\nu U/h^2} \sim \frac{g\alpha\Delta T}{\nu\kappa/h^3} = \frac{\alpha \Delta T g h^3}{\nu\kappa} = \mathrm{Ra}.$$

For the boundary conditions, (13), we apply a similar tranformation and get

$$\begin{cases} \bar{T}(\bar{\boldsymbol{x}}, \bar{t})|_{\bar{y}=0} = 0, & -\infty < \bar{x}, \bar{z} < \infty, \bar{t} > 0, \\ \bar{T}(\bar{\boldsymbol{x}}, \bar{t})|_{\bar{y}=1} = 1, & -\infty < \bar{x}, \bar{z} < \infty, \bar{t} > 0, \\ \bar{\boldsymbol{u}}(\bar{\boldsymbol{x}}, \bar{t})|_{\bar{y}=0} = \bar{\boldsymbol{u}}(\bar{\boldsymbol{x}}, \bar{t})|_{\bar{y}=1} = \boldsymbol{0}, & -\infty < \bar{x}, \bar{z} < \infty, \bar{t} > 0. \end{cases} \tag{19}$$

5 Stability analysis in two dimensions

An important aspect of a flow is the stability, i.e. the effect that a disturbance has on a given state. If a perturbation is introduced and it is allowed to grow up to a finite amplitude the flow might enter a new state. Further disturbances may be able to be introduced in this state and as the disturbances adds up the flow can reach a chaotic state, normally known as turbulence.

In this section the stability of the governing equations derived in the previous chapters will be examined using linear stability analysis. An introduction to this method, called normal mode analysis, will be presented and the equations will be rewritten in a number of steps. Finally a condition will be derived for the limit where the flow transitions from being stable to unstable. The analysis will be limited to two dimensions, streamwise and wall-normal.

5.1 Linear stability analysis and the method of normal modes

The general idea of linear stabilitiy analysis is to introduce an infinitesimal perturbation to a background state and examine whether its amplitude grows or decays with time. Since the perturbations are small the equations can be linearized which eases the analysis. The drawback of this method is that it only considers the initial development of the disturbance. Nevertheless, we will see that the results found in this section agrees very well with the results of the numerical experiments conducted in section 6.

In the method of normal modes the perturbations are assumed to be sinusoidal. As we will see later, the allowed perturbations will take the form

$$f = \hat{f}(y) e^{ikx + \sigma t}$$

where f is an arbitrary perturbation with complex amplitude $\hat{f}$, wave number k in the x-direction and growth rate σ. The development in time of the solution will thus only depend on the sign of the real part of σ, here denoted σ_r.

- If $\sigma_r > 0$ the perturbation will grow with time, unstable solution
- If $\sigma_r < 0$ the perturbation will decay with time, stable solution
- $\sigma_r = 0$ is the so-called marginally stable case, i.e. the boundary between stability and instability.

The linearity of the equations yields that any possible disturbance can be expressed as a superpositions of these perturbations. If we can show that for any given k, the solution is stable, then the solution will be stable for any infinitesimal disturbance.

5.2 Eliminating the pressure term from the governing equations

The governing equations from last section will now be treated. Please note that since we will only consider non-dimensional quantities from now on we will drop the overbar.

We have no information about the pressure distribution in the fluid and therefore we want to eliminate the pressure gradient from equation (18). Using the vector identity [2]

$$\boldsymbol{u} \cdot \nabla \boldsymbol{u} = \nabla \left(\frac{\boldsymbol{u} \cdot \boldsymbol{u}}{2} \right) + \boldsymbol{\omega} \times \boldsymbol{u},$$

and inserting it into equation (18) yields

$$\frac{1}{\mathrm{Pr}} \left[\frac{\partial \boldsymbol{u}}{\partial t} + \nabla \left(\frac{\boldsymbol{u} \cdot \boldsymbol{u}}{2} \right) + \boldsymbol{\omega} \times \boldsymbol{u} \right] = -\nabla p + \mathrm{Ra} T \boldsymbol{e}_y + \nabla^2 \boldsymbol{u}. \tag{20}$$

Taking the curl of this equation and using that the curl of a gradient is equal to zero, we get

$$\frac{1}{\mathrm{Pr}} \left[\frac{\partial}{\partial t} (\nabla \times \boldsymbol{u}) + \nabla \times \boldsymbol{\omega} \times \boldsymbol{u} \right] = \nabla \times \mathrm{Ra} T \boldsymbol{e}_y + \nabla^2 (\nabla \times \boldsymbol{u}). \tag{21}$$

Identifying the vorticity $\boldsymbol{\omega} = \nabla \times \boldsymbol{u}$ and applying $\nabla \times \boldsymbol{\omega} \times \boldsymbol{u} = \boldsymbol{u} \cdot \nabla \boldsymbol{\omega} - \boldsymbol{\omega} \cdot \nabla \boldsymbol{u}$ [2] yields

$$\frac{1}{\mathrm{Pr}} \left[\frac{\partial \omega}{\partial t} + \boldsymbol{u} \cdot \nabla \boldsymbol{\omega} - \boldsymbol{\omega} \cdot \nabla \boldsymbol{u} \right] = \nabla \times \mathrm{Ra} T \boldsymbol{e}_y + \nabla^2 \omega. \tag{22}$$

We will only consider the two-dimensional case, $T = T(x, y, t)$ and $\boldsymbol{u} = u_x(x, y, t)\boldsymbol{e}_x + u_y(x, y, t)\boldsymbol{e}_y$, hence

$$\begin{aligned}
&\boldsymbol{\omega} = \left(\frac{\partial u_y}{\partial x} - \frac{\partial u_x}{\partial y}\right)\boldsymbol{e}_z = \omega \boldsymbol{e}_z \\
&\boldsymbol{\omega} \cdot \nabla \boldsymbol{u} = 0 \\
&\nabla \times T\boldsymbol{e}_y = \frac{\partial T}{\partial x}\boldsymbol{e}_z.
\end{aligned}$$

From this we get

$$\begin{cases}
\dfrac{1}{\mathrm{Pr}}\left[\dfrac{\partial \omega}{\partial t} + \boldsymbol{u} \cdot \nabla \boldsymbol{\omega}\right] = \mathrm{Ra}\dfrac{\partial T}{\partial x} + \nabla^2 \omega \\
\dfrac{\partial T}{\partial t} + \boldsymbol{u} \cdot \nabla T = \nabla^2 T.
\end{cases} \tag{23}$$

These equations do not contain the pressure term any longer.

5.3 Linearization

Consider small disturbances, $\boldsymbol{u}'$, T' and ω' from a background state , $\tilde{\boldsymbol{u}} = \boldsymbol{0}$, $\tilde{T} = \tilde{T}(y)$ and $\tilde{\omega} = 0$. The background temperature field, $\tilde{T}(y)$, is found from (23) by setting $\boldsymbol{u} = \boldsymbol{0}$ and $\omega = 0$, thus yielding

$$\nabla^2 \tilde{T}(y) = \frac{\partial^2 \tilde{T}}{\partial y^2} = 0, \tag{24}$$

applying the boundary conditions $T(0) = 0, T(1) = 1$ gives the solution

$$\tilde{T}(y) = y. \tag{25}$$

By inserting $T = \tilde{T}(y) + T'$, $\boldsymbol{u} = \boldsymbol{u}'$ and $\omega = \omega'$ into (23) and linearizing by neglecting higher order terms, the equations for the disturbances are found to be

$$\begin{cases}
\dfrac{1}{\mathrm{Pr}}\dfrac{\partial \omega'}{\partial t} = \mathrm{Ra}\dfrac{\partial T'}{\partial x} + \nabla^2 \omega' \\
\dfrac{\partial T'}{\partial t} + u_y = \nabla^2 T'.
\end{cases} \tag{26}$$

5.4 Streamfunction form

We currently have three unknowns (ω', u_y' and T') and the three equations ((26) and the continuity equation $\nabla \cdot \boldsymbol{u}' = \boldsymbol{0}$). In order to reduce the number of unknown variables we introduce the stream function, ψ', defined by

$$u_x' = \frac{\partial \psi'}{\partial y}, \quad u_y' = -\frac{\partial \psi'}{\partial x}, \tag{27}$$

which replaces the continuity equation.

The vorticity then takes the form $\omega = -\nabla^2\psi$ and upon substitution into (26) the resulting governing equations become

$$\begin{cases} \dfrac{1}{\mathrm{Pr}}\dfrac{\partial}{\partial t}\nabla^2\psi' = -\mathrm{Ra}\dfrac{\partial T'}{\partial x} + \nabla^2(\nabla^2\psi') \\ \dfrac{\partial T'}{\partial t} - \dfrac{\partial \psi'}{\partial x} = \nabla^2 T'. \end{cases} \tag{28}$$

The boundary conditions transform to

$$\begin{aligned} u_x(0) = u_y(0) = \frac{\partial u_y}{\partial y}(0) = 0 \quad &\Longrightarrow \quad \frac{\partial \psi}{\partial y}(0) = 0 \\ u_x(1) = u_y(1) = \frac{\partial u_y}{\partial y}(1) = 0 \quad &\Longrightarrow \quad \frac{\partial \psi}{\partial y}(1) = 0 \\ T(0) = 0, \quad T(1) = 1, \quad T' = T - \tilde{T} \quad &\Longrightarrow \quad T'(0) = T'(1) = 0. \end{aligned}$$

5.5 Forming the eigenvalue problem

The set of differential equations (28) is linear and the coefficients do neither depend on x nor t. This allow us to make the following normal mode ansatz for ψ' and T'

$$\begin{aligned} \psi' &= \hat{\psi}(y)e^{ikx+\sigma t} \\ T' &= \hat{T}(y)e^{ikx+\sigma t}, \end{aligned}$$

where $\hat{\psi}$ and $\hat{T}$ are the complex amplitudes of ψ' and T', k is the wavenumber and σ is the growth rate. Insertion into the governing equations yields

$$\begin{cases} \dfrac{1}{\mathrm{Pr}}\sigma\left[\dfrac{\mathrm{d}^2}{\mathrm{d}y^2} - k^2\right]\hat{\psi} = -\mathrm{Ra}ik\hat{T} + \left[\dfrac{\mathrm{d}^2}{\mathrm{d}y^2} - k^2\right]^2\hat{\psi}, \\ \sigma\hat{T} - ik\hat{\psi} = \left[\dfrac{\mathrm{d}^2}{\mathrm{d}y^2} - k^2\right]\hat{T}. \end{cases} \tag{29}$$

σ and k can be shown to be real [2]. The sign of σ will, as previously stated, determine whether the solution is stable or not.

Consider the limit between these cases, $\sigma = 0$, the so-called marginally stable case. This case can only be consistent with the governing equations if

$$\begin{cases} 0 = -\mathrm{Ra}ik\hat{T} + \left[\dfrac{\mathrm{d}^2}{\mathrm{d}y^2} - k^2\right]^2\hat{\psi}, \\ -ik\hat{\psi} = \left[\dfrac{\mathrm{d}^2}{\mathrm{d}y^2} - k^2\right]\hat{T}. \end{cases} \tag{30}$$

Solving for $\hat{T}$ in the first and sustituting into the second yields

$$-ik\hat{\psi} = \left[\frac{\mathrm{d}^2}{\mathrm{d}y^2} - k^2\right] \frac{1}{\mathrm{Ra}ik} \left[\frac{\mathrm{d}^2}{\mathrm{d}y^2} - k^2\right]^2 \hat{\psi}, \tag{31}$$

which can be simplified to

$$k^2\hat{\psi} = \frac{1}{\mathrm{Ra}} \left[\frac{\mathrm{d}^2}{\mathrm{d}y^2} - k^2\right]^3 \hat{\psi}. \tag{32}$$

This forms an eigenvalue problem with eigenvalue Ra and eigenfunction $\hat{\psi}$. The eigenvalues for a given k will give thus give the Rayleigh numbers yielding a neutrally stable solution of the equations of motion.

In order to be able to find the possible solutions, the boundary conditions must be transformed again

$$T'(0) = T'(1) = 0 \quad \Longrightarrow \quad \hat{T}(0) = \hat{T}(1) = 0, \tag{33}$$

$$\frac{\partial\psi}{\partial y}(0) = \frac{\partial\psi}{\partial y}(1) = 0 \quad \Longrightarrow \quad \frac{d\hat{\psi}}{dy}(0) = \frac{d\hat{\psi}}{dy}(1) = 0. \tag{34}$$

The two last boundary conditions are found by considering (30) and using (33), resulting in

$$\left[\frac{\mathrm{d}^2}{\mathrm{d}y^2} - k^2\right]^2 \hat{\psi}(0) = \left[\frac{\mathrm{d}^2}{\mathrm{d}y^2} - k^2\right]^2 \hat{\psi}(1) = 0. \tag{35}$$

5.6 Solving the eigenvalue problem

The equation (32) is a linear homogenous ODE with constant coefficients and we can make the ansatz $\hat{\psi}(y) = e^{qy}$, where q is a constant. By inserting this into the equation (32) we get

$$k^2 + \frac{1}{Ra}\left[q^2 - k^2\right]^3 = 0, \tag{36}$$

which has the six roots

$$\begin{cases} iq_0 = \pm ik\left(-1 + \left(\frac{Ra}{k^4}\right)^{1/3}\right)^{1/2} \\ q_1 = \pm k\left(1 + \left(\frac{Ra}{k^4}\right)^{1/3}\left(\frac{1}{2} + i\frac{\sqrt{3}}{2}\right)\right)^{1/2} \\ q_2 = \pm k\left(1 + \left(\frac{Ra}{k^4}\right)^{1/3}\left(\frac{1}{2} - i\frac{\sqrt{3}}{2}\right)\right)^{1/2}, \end{cases} \tag{37}$$

and the solution takes the form

$$\hat{\psi}(y) = Ae^{q_0 y} + Be^{-q_0 y} + Ce^{q_1 y} + De^{-q_1 y} + Ee^{q_2 y} + Fe^{-q_2 y} \tag{38}$$

where A, B, C, D, E and F are constants. The boundary conditions (33)-(35) demand that

$$\begin{cases} \hat{\psi}(0) = A + B + C + D + E + F = 0 \\ \hat{\psi}(1) = Ae^{q_0} + Be^{-q_0} + Ce^{q_1} + De^{-q_1} + Ee^{q_2} + Fe^{-q_2} = 0 \\ \hat{\psi}'(0) = Aq_0 - Bq_0 + Cq_1 - Dq_1 + Eq_2 - Fq_2 = 0 \\ \hat{\psi}'(1) = Aq_0e^{q_0} - Bq_0e^{-q_0} + Cq_1e^{q_1} - Dq_1e^{-q_1} + Eq_2e^{q_2} - Fq_2e^{-q_2} = 0 \\ \left[\frac{d^2}{dy^2} - k^2\right]^2 \hat{\psi}(0) = (q_0^2 - k^2)^2 A - (q_0^2 - k^2)^2 B - (q_1^2 - k^2)^2 C \\ \quad -(q_1^2 - k^2)^2 D - (q_2^2 - k^2)^2 E - (q_2^2 - k^2)^2 E = 0 \\ \left[\frac{d^2}{dy^2} - k^2\right]^2 \hat{\psi}(1) = (q_0^2 - k^2)^2 Ae^{q_0} - (q_0^2 - k^2)^2 Be^{q_0} - (q_1^2 - k^2)^2 Ce^{q_1} \\ \quad -(q_1^2 - k^2)^2 De^{q_1} - (q_2^2 - k^2)^2 Ee^{q_2} - (q_2^2 - k^2)^2 Ee^{q_2} = 0. \end{cases} \tag{39}$$

In order to find the non-trivial solutions to this system of equations we write it on matrix form, $M\mathbf{b} = \mathbf{0}$, where

$$M^T = \begin{pmatrix} 1 & e^{q_0} & q_0 & q_0e^{q_0} & (q_0^2 - k^2)^2 & (q_0^2 - k^2)^2 e^{q_0} \\ 1 & e^{-q_0} & -q_0 & -q_0e^{-q_0} & (q_0^2 - k^2)^2 & (q_0^2 - k^2)^2 e^{-q_0} \\ 1 & e^{q_1} & q_1 & q_1e^{q_1} & (q_1^2 - k^2)^2 & (q_1^2 - k^2)^2 e^{q_1} \\ 1 & e^{-q_1} & -q_1 & -q_1e^{-q_1} & (q_1^2 - k^2)^2 & (q_1^2 - k^2)^2 e^{-q_1} \\ 1 & e^{q_2} & q_2 & q_2e^{q_2} & (q_2^2 - k^2)^2 & (q_2^2 - k^2)^2 e^{q_2} \\ 1 & e^{-q_2} & -q_2 & -q_2e^{-q_2} & (q_2^2 - k^2)^2 & (q_2^2 - k^2)^2 e^{-q_2} \end{pmatrix}, \quad \mathbf{b} = \begin{pmatrix} A \\ B \\ C \\ D \\ E \\ F \end{pmatrix},$$

and solve for a zero-determinant of M.

The equation $\det(M) = 0$ was solved numerically for a range of fix values of k. When k is fix the value of M depends solely on the value of the Rayleigh number yielding a one-dimensional equation $\det(M(\mathrm{Ra}))|_k = 0$. This equation was solved in MATLAB using Newton's method which, given a start guess Ra_0, applies the following iteration scheme

$$\mathrm{Ra}_{n+1} = \mathrm{Ra}_n - \frac{d(\mathrm{Ra}_n)}{d'(\mathrm{Ra}_n)},$$

where we have let $d = \det(M)$ for brewity.

The derivative, $d'(\mathrm{Ra})$, was evaluated using a difference approximation on the form

$$d'(\mathrm{Ra}) \approx \frac{d(\mathrm{Ra} + \Delta) - d(\mathrm{Ra} - \Delta)}{2\Delta}$$

where Δ was choosen to be small.

The complete code can be found in appendix A and the result for a range of k-values are presented in figure 2. We can see the highest Rayleigh number yielding a stable solution for all values of k is $\mathrm{Ra} = 1708$.

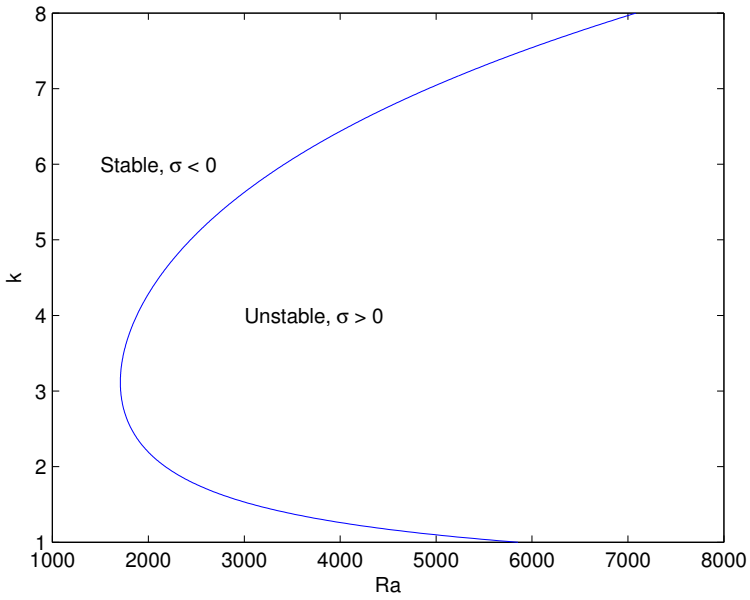

Figure 2: Stability region

6 Simulations

In this section, the previously derived equations will be solved using Simson [1], a code developed at KTH Mechanics during the last 20 years. The numerical method will be introduced briefly and the derived analytic conditions for stability will be compared to numerical results in two-dimensional simulations. Different solutions in two and three dimensions will also be presented and discussed.

6.1 Formulation of the numerical problem

The starting point for the numerical simulations are the set of equations (17) from section 4 and the continuity equation. However, the infinite region is replaced by a finite domain

$$\Omega = \{(x, y, z)\ ;\ 0 < x < L_x, -1 < y < 1, 0 < z < L_z\}.$$

where L_x and L_z are the dimensions of the domain in the x- and z-direction. We have that

$$\begin{cases} \dfrac{\mathrm{D}\boldsymbol{u}}{\mathrm{D}t} = -\mathrm{Pr}\nabla p + \mathrm{Ri}\alpha\Delta T T\boldsymbol{e}_y + \dfrac{1}{\mathrm{Re}}\nabla^2\boldsymbol{u}, & \boldsymbol{x}\in\Omega,\ t>0, \\ \dfrac{\mathrm{D}t}{\mathrm{D}t} = \dfrac{1}{\mathrm{Pe}}\nabla^2 t, & \boldsymbol{x}\in\Omega,\ t>0, \\ \nabla\cdot\boldsymbol{u} = 0, & \boldsymbol{x}\in\Omega,\ t>0, \end{cases}$$

The boundary conditions in the x- and z-directions are replaced by periodicity, yielding

$$\begin{cases} T(\boldsymbol{x},t)|_{y=0} = T_0, & x\in[0,L_x],\ z\in[0,L_z],\ t>0, \\ T(\boldsymbol{x},t)|_{y=h} = T_1, & x\in[0,L_x],\ z\in[0,L_z],\ t>0, \\ \boldsymbol{u}(\boldsymbol{x},t)|_{y=0} = \boldsymbol{u}(\boldsymbol{x},t)|_{y=h} = \boldsymbol{0}, & x\in[0,L_x],\ z\in[0,L_z],\ t>0, \\ \boldsymbol{u}(\boldsymbol{x},t) = \boldsymbol{u}(\boldsymbol{x}+L_x\boldsymbol{e}_x,t), & y\in[-1,1],\ z\in[0,L_z],\ t>0, \\ \boldsymbol{u}(\boldsymbol{x},t) = \boldsymbol{u}(\boldsymbol{x}+L_z\boldsymbol{e}_z,t), & x\in[0,L_x],\ y\in[0,L_x],\ t>0. \end{cases}$$

The intial conditions used are a linear temperature distribution and a velocity field with random noise, $\boldsymbol{u}_0(\boldsymbol{x})$, satisfying the continuity equation, hence

$$\begin{cases} T(y,0)|_{t=0} = T_0 + \frac{y}{h}(T_1 - T_0), & \boldsymbol{x}\in\Omega, \\ \boldsymbol{u}(\boldsymbol{x},0)|_{t=0} = \boldsymbol{u}_0(\boldsymbol{x}), & \boldsymbol{x}\in\Omega. \end{cases}$$

6.2 Introduction to the numerical method of Simson

Simson is a pseudo-spectral solver for incompressible flows. The solver applies a Fourier expansion of the solution in the span- and streamwise directions and an expansion in Chebychev polynomials in the normal direction. Time is discretized using a combination of the Crank-Nicholson and Runge-Kutta iteration schemes. To avoid having to evaluate the convolution appearing from the non-linear terms in the differential equations at each time step this value is calculated in physical space and then transformed back into Fourier-Chebychev space. For more information about the solution scheme, see Chevalier, Schlatter, Lundbladh and Henningson [1].

6.3 Simulations in two dimensions

6.3.1 Numerical stability analysis

The stability criteria found in section 5 will now be verified by numerical experiments conducted with Simson. The resolution used in the experiments are 32 and 33 spectral modes in the x- and y-direction respectively.

Since we have periodic boundary conditions, the wavenumbers for the normal modes in two dimensions will be a multiple of $2\pi/L_x$ where L_x is the length of the domain in the x-direction. This allows us to set a value of k for which the limiting value of the Rayleigh number can be found.

The procedure used was first choosing a value of Ra and then making simulations for different k:s until the limit of stability was found. This was done for nine different values of Ra. The values found are plotted together with the curve found in section 5 in figure 3. We were however unable to obtain results for $k < 2$ since the numerical method failed to converge in this case.

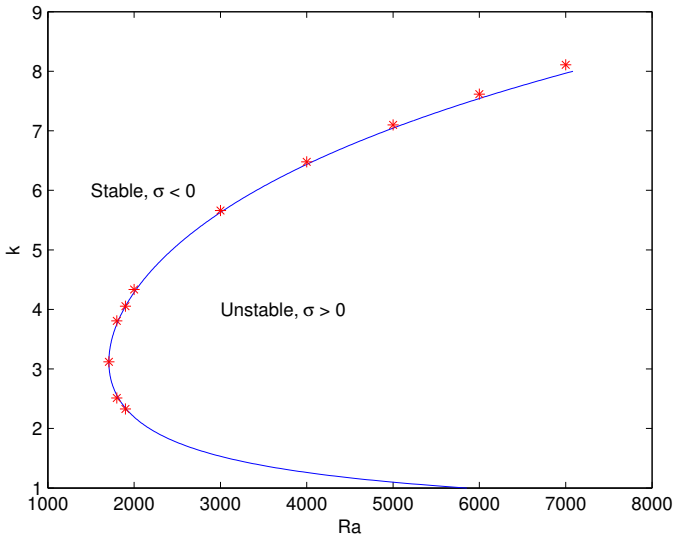

Figure 3: Stability region with numerically found values.

In figure 3 we can observe the lowest value of the Rayleigh number on the stability limit is Ra $= 1708$ for $k = 3.12$. This means that we will have a stable flow for all k-values where Ra < 1708. An illustration of the temperature and velocity in the x-direction at this point is presented in figure 4. The temperature is here linearly distributed vertically, the velocity field though has small values. To know if the flow is stable for this Rayleigh number we will have to investigate if the velocity field increases or decreases with time i.e. if the growth rate σ_r is positive or negative. To see this $\log u_{rms}$ and $\log v_{rms}$ was plotted against time for some Rayleigh numbers around 1708. The slope of these curves gives σ_r, as discussed in the stability section. In figure 5 we can see that for Ra $= 1707$ $\sigma_r < 0$, the velocity goes to zero and we have a stable solution. For Ra $= 1708$ $\sigma_r > 0$ and we have an unstable solution. The conclusion is that the limit $\sigma_r = 0$ lies between these two Rayleigh numbers and we have a stable flow for Ra < 1708.

6.3.2 Discussion of results for simulation with different Rayleigh numbers

It is also interesting to investigate the behavior of the fluid for different Rayleigh numbers. Studies where made for a fix k-value, $k \approx 2.24$ and Ra $= 1000, 4000$ and 10000. For the higher Rayleigh numbers the non-linearity is expected to play an important role, leading to a so-called saturated state. All of the plots of these simulations are for 70 time units.

For Ra $= 1000$ we would expect, as concluded earlier, a stable flow. The temperature and velocity distibution can be seen in figure 6. Here we can see that just as for Ra $= 1708$ the temperature is linearly distributed vertically while we have a small irregular velocity field.

For Ra $= 4000$ we obtained a more unstable flow, as can bee seen in figure 7. The higher ratio between bouyancy and viscous forces results in this wave-shaped temperature distribution. We can also see on the velocity level curves that we now have a flow with clear two-dimensional rolls in the velocity field.

The last study is for Rayleigh number, Ra $= 10000$. In figure 12 we can see the characteristic mushroomed-shaped temperature distributions and a high velocity in the flow.

To better understand how the velocity is distributed we also plot the velocity field in the x-y-plane. In figure 9 we can see the vector fields for Ra $= 1000, 4000$ and 10000. For Ra $= 1000$ we only have a small random motion due to the decaying effect of the initial random disturbances. For Ra $= 4000$ and 10000 the fluid is circulating and as the length of the arrows indicates we have a much higher velocity for the higher Rayleigh number.

6.4 Simulations in three dimensions

Simson was also used for simulating the flow in three dimensions for different values of the Rayleigh number. The resolution was now incresed to 64 spectral nodes in the x- and z-directions and 33 in the y-direction. For Rayleigh numbers in the region $2000 \leq \text{Ra} \leq 5000$ we observed that the flow converged to convection rolls in the velocity field and the characteristic mushrooms in the temperature field. Examples of this can be seen in figure 10 where temperature distribution and streamlines of the flow are shown. This agrees well with theory that states that stationary patterns should occur when the kinetic energy generated due to the cooling and heating of the plates is balanced by viscous dissipation [2].

For Ra $= 4500$ and 4750 the flow never converged for a $L_x = L_z = 10$ simaluation area, but when it was increased to $L_x = L_z = 20$ the flow converged to rolls. This could be because the domain was too small with $L_x = L_z = 10$ which inhibited the growth of the rolls with the proper wavelength.

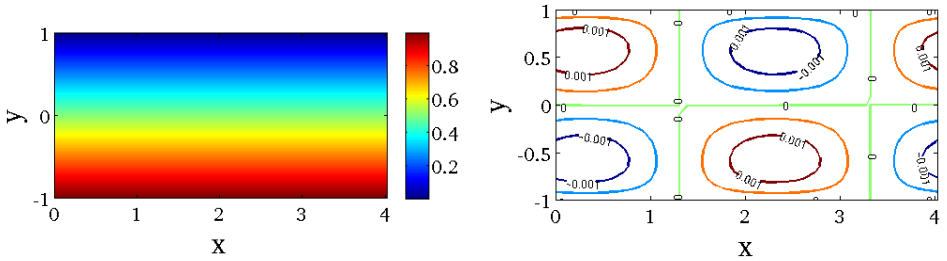

(a) T (b) u

Figure 4: Level curves for T and u for $\mathrm{Ra} = 1708, k \approx 3.12$.

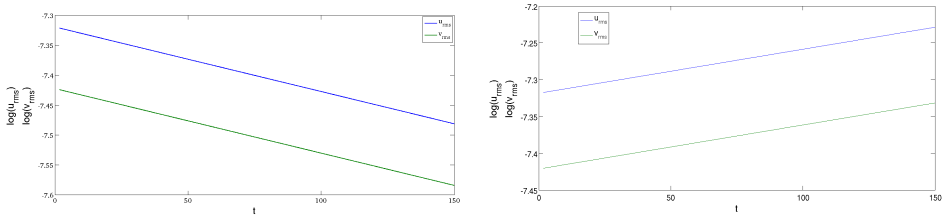

(a) $\mathrm{Ra} = 1707$ (b) $\mathrm{Ra} = 1708$

Figure 5: Plots of $\log u_{rms}$ and $\log v_{rms}$.

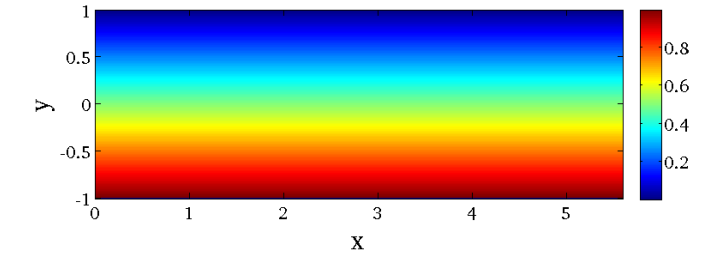

(a) T

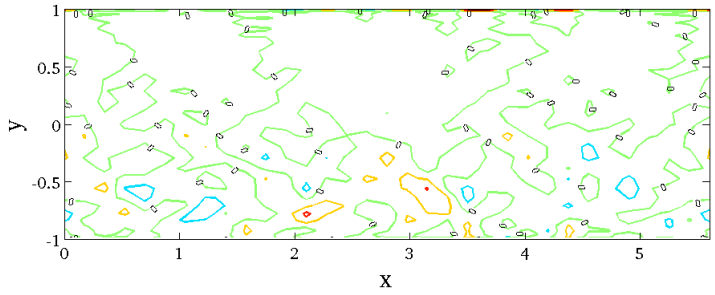

(b) u

Figure 6: Level curves for T and u for $\mathrm{Ra} = 1000$.

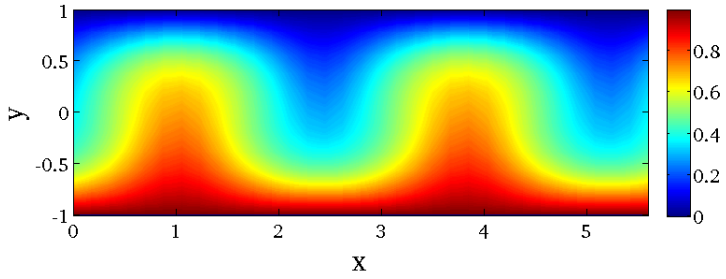

(a) T

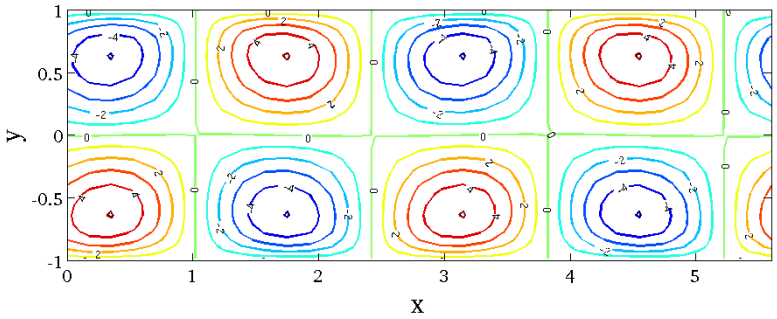

(b) u

Figure 7: Level curves for T and u for Ra $= 4000$.

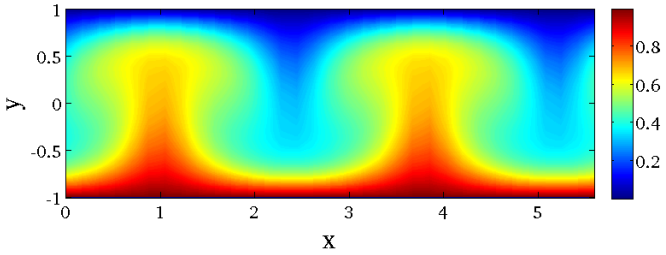

(a) T

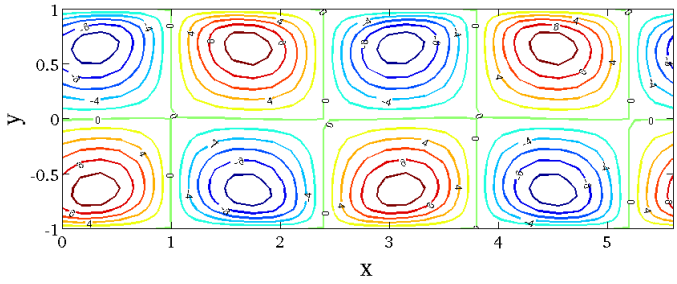

(b) u

Figure 8: Level curves for T and u for Ra $= 10000$.

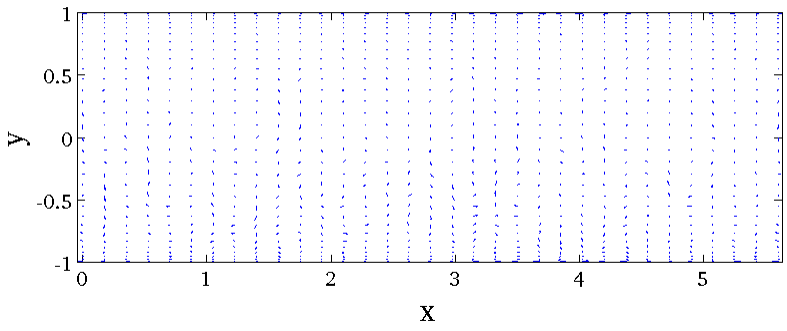

(a) Ra = 1000

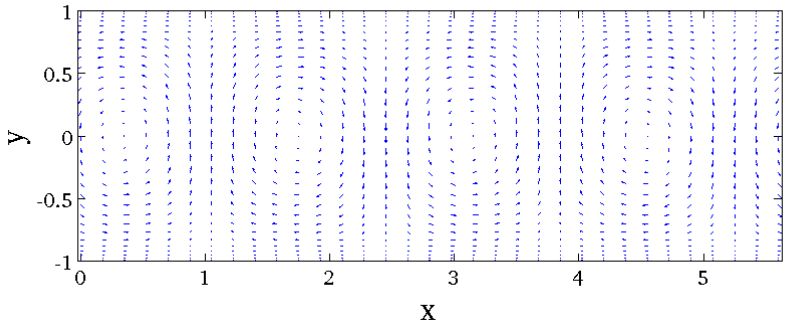

(b) Ra = 4000

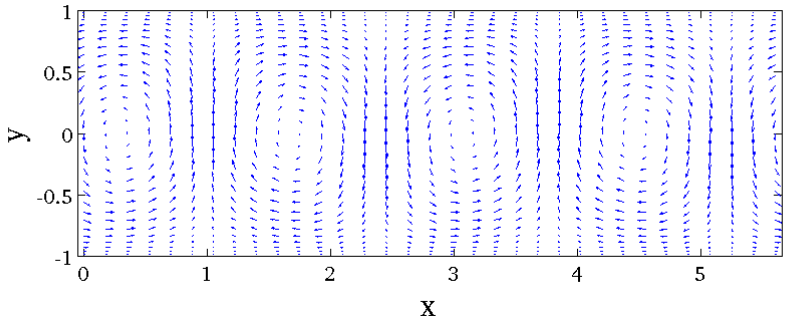

(c) Ra = 10000

Figure 9: Velocity fields for three different values of Ra.

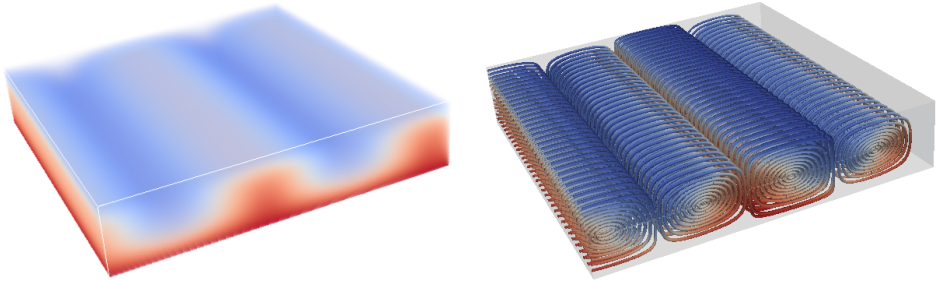

(a) Temperature distribution (b) Streamlines

Figure 10: Ra = 3000.

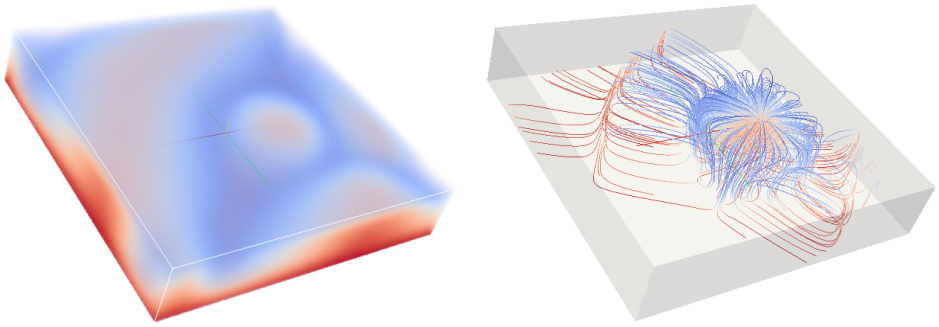

(a) Temperature distribution (b) Streamlines

Figure 11: Ra = 4500.

For higher Rayleigh numbers, in the region $5000 < \text{Ra} \leq 10000$, the flow never converged into a stationary pattern. Instead, the pattern took an oscillating sinusodial form, which can be seen in figure 12.

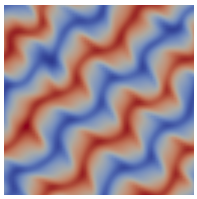

(a) Temperature distribution over the center plane.

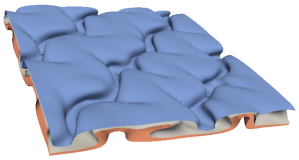

(b) Isocontours for the temperature field.

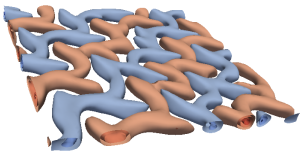

(c) Isocontours for the velocity in the normal direction.

Figure 12: $\text{Ra} = 10000$ simulated over a $L_x = L_z = 20$ area.

When the Rayleigh number reached 20000 the motion was initially totally random, but after some time it merged into travelling wave-like patterns. Illustrations of the temperature field at $\text{Ra} = 20000$ is presented in figure 13. This simulation was done with 128 spectral nodes in the x- and z-directions and 65 in the y-direction.

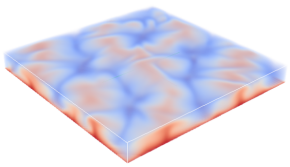

(a) 30 time units

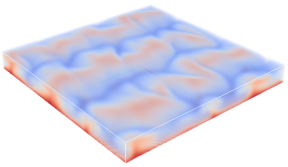

(b) 60 time units

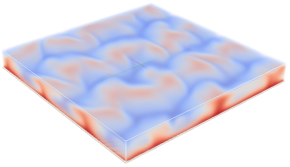

(c) 90 time units

Figure 13: $\text{Ra} = 20000$ for three time units.

For higher Rayleigh numbers a less structured flow will appear and turbulence will occur at $\text{Ra} > 50000$ [2].

6.4.1 Flow patterns

We have seen that the unstable flow can converge into stationary flow patterns. The most commonly occuring flow pattern in our simulations is convections rolls but other patterns such as hexagonal convections cells may also occur. The hexagonal cells often occur in the beginning of a simulation and then merge into convetion rolls. Since the problem is horizontally isotropic the convection patterns will form in a horizontally random direction i.e. either in the x-, z- or a diagonal direction. This can be seen if you compare figure 10 and figure 14 where the rolls have lined up in different directions. An example of a hexagonal cell can be seen in figure 11. In this example a point source located in the middle of the hexagonal cell was used to visualise the streamlines.

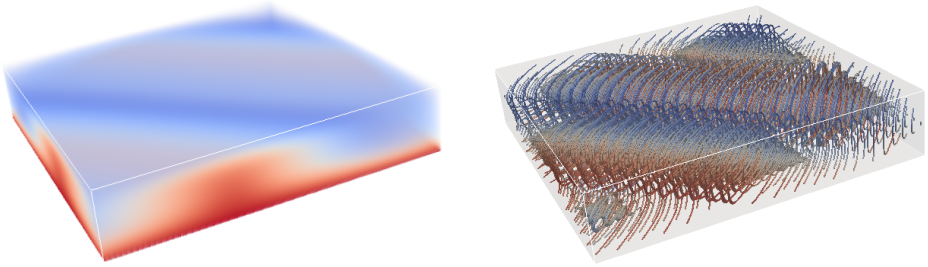

(a) Temperature distribution (b) Streamlines

Figure 14: Ra = 5000.

7 Conclusion

The general behavior of the fluid, in the aspect of Rayleigh-Bénard, is only governed by the dimensionless Rayleigh number. The stability analysis showed that the flow will be stable for any wavenumber if the Rayleigh number is smaller than 1708, this was later verified by the numerical simulations. The analytically derived stability curve agrees well with the stability found numerically. This implies that the linear stability analysis is accurate and a good model to predict the behavior of the flow.

The Rayleigh number also affected other aspects of the flow. We saw that when the Rayleigh number was $2000 \leq \mathrm{Ra} \leq 5000$ the flow converged to convection rolls which are steady and strictly two-dimensional, when $5000 < \mathrm{Ra} \leq 10000$ these rolls oscillated in a sinusodial way instead of converging to a steady pattern. For $\mathrm{Ra} = 20000$ the behavior of the flow became totally random at first but eventually took a more structured form. An increasing Rayleigh number resulted in higher velocities and less structured flow patterns.

A MATLAB code for the stability curve

The value of $\det(M)$ is calculated with the following function

```
function ret = detA(Ra)
    global k
    q0= 1i*k*(-1+(Ra/k^4)^(1/3))^(1/2);
    q1= k*(1+(Ra/k^4)^(1/3)*(1/2+1i*sqrt(3)/2))^(1/2);
    q2= k*(1+(Ra/k^4)^(1/3)*(1/2-1i*sqrt(3)/2))^(1/2);

    A=[1 1 1 1 1 1
        exp(q0) exp(-q0) exp(q1) exp(-q1) exp(q2)
            exp(-q2)
        q0 -q0 q1 -q1 q2 -q2
        q0*exp(q0) -q0*exp(-q0) q1*exp(q1) -q1*exp(-q1)
            q2*exp(q2) -q2*exp(-q2)
        (q0^2-k^2)^2 (q0^2-k^2)^2 (q1^2-k^2)^2
            (q1^2-k^2)^2 (q2^2-k^2)^2 (q2^2-k^2)^2
        (q0^2-k^2)^2*exp(q0) (q0^2-k^2)^2*exp(-q0)
            (q1^2-k^2)^2*exp(q1) (q1^2-k^2)^2*exp(-q1)
            (q2^2-k^2)^2*exp(q2) (q2^2-k^2)^2*exp(-q2)];
    ret=det(A);
end
```

and is thereafter used in the following program to find the solution of $\det(M) = 0$ for a range of values of k in the interval $[1, 8]$.

```
clear, clf, clc
global k

ks=8:-0.01:1; %range of ks to solve for
Ra=7000; %start guess for k = 8
delta_Ra = 0.001; %step size for derivative
    approximation
tolerance = 0.001; %tolerance for the absolute error
    of Ra
Result=[]; %vector for results

for k=ks
    dR = 1; %dummy value
    %Solve with Newton's method until the absolute
        value error
    %approximation dR reaches a value below the
        tolerance
    while abs(dR) > tolerance
        f = detA(Ra);
        df =
            (detA(Ra+delta_Ra)-detA(Ra-delta_Ra))/(2*delta_Ra);
        dR = - f/df;
        Ra = Ra + dR;
    end
```

```
20        Result=[Result Ra];
21    end
22    plot(Result,ks)
23    xlabel('Ra'), ylabel('k')
```

References

[1] M. Chevalier, P. Schlatter, A. Lundbladh, and D. Henningson. Simson - a pseudo-spectral solver for incompressible boundary layer flows. Technical report, KTH Mechanics, 2007.

[2] P. K. Kundu and I. M. Cohen. *Fluid Mechanics*. Academic press, 4th edition, 2008.

[3] E. A. Spiegel and G. Veronis. On the boussinesq appoximation for a compressible fluid. *Astrophysical Journal*, 131:442–447, 1960.